The Journal of Chemical Physics

Surface solvation and hindered isomerization at the water/silica interface explored with second harmonic generation

Cite as: J. Chem. Phys. **150**, 194701 (2019); https://doi.org/10.1063/1.5066451
Submitted: 15 October 2018 . Accepted: 18 April 2019 . Published Online: 16 May 2019

Grace E. Purnell, and Robert A. Walker

The Journal of Chemical Physics ARTICLE scitation.org/journal/jcp

Surface solvation and hindered isomerization at the water/silica interface explored with second harmonic generation

Cite as: J. Chem. Phys. 150, 194701 (2019); doi: 10.1063/1.5066451
Submitted: 15 October 2018 • Accepted: 18 April 2019 •
Published Online: 16 May 2019

Grace E. Purnell[1] and Robert A. Walker[1,2,a)]

AFFILIATIONS

[1] Department of Chemistry and Biochemistry, Montana State University, Bozeman, Montana 59717, USA
[2] Montana Materials Science Program, Montana State University, Bozeman, Montana 59717, USA

Note: This article is part of the Special Topic "Nonlinear Spectroscopy and Interfacial Structure and Dynamics" in J. Chem. Phys.
[a)] **Author to whom correspondence should be addressed:** rawalker@montana.edu. Telephone: +1 (406) 994–7928.

ABSTRACT

Resonantly enhanced second harmonic generation (SHG) spectra of Coumarin 152 (C152) adsorbed at the water-silica interface show that C152 experiences a local dielectric environment slightly more polar than that of bulk water. This result stands in contrast to recently reported time-resolved fluorescence experiments and simulations that suggest an alkane-like permittivity for interfacial water at strongly associating, hydrophilic solid surfaces. Taken together, these results imply that while the static electric field across the aqueous-silica interface may be large, restricted water dynamics lead to apparent nonpolar solvation behavior similar to that experienced by solutes in confinement. Resonance-enhanced SHG spectra and time-resolved fluorescence of C152 adsorbed to aqueous-hydrophobic silica surfaces show that when water's ability to hydrogen bond with the silica surface is eliminated, a solute's interfacial solvation and corresponding ability to photoisomerize converge to an intermediate limit similar to that experienced in bulk acetone or methanol. While water structure and dynamics at solid-liquid interfaces have received considerable attention, results presented below show how strong solvent-substrate interactions can create conflicting pictures of solute reactivity across buried interfaces.

I. INTRODUCTION

Water's complicated behavior at surfaces has attracted significant attention since the first nonlinear spectroscopic study of water's interfacial vibrational structure was published in the early 1990s.[1] In parallel, numerous studies of organic solvents at interfaces have shown that surfaces can significantly change the organization and properties of adjacent liquids from bulk solution limits.[2–6] For example, nonlinear optical experiments examining the silica-methanol interface showed conclusively that this interface is characterized by a distinctly nonpolar solvation region where the effective dielectric constant is ~2 (compared to methanol's bulk static dielectric constant $\varepsilon = 32.7$).[7] Molecular dynamics simulations and complementary vibrational spectroscopy studies suggest that at the silica-methanol interface, solvent density is significantly reduced within ~1 nm of the interface, and the interfacial methanol solvent molecules create a bilayer-type structure where methyl groups in adjacent methanol solvent layers adopt antiparallel orientation.[7] This organization creates an alkane-like sheet adjacent to the interface with a correspondingly low dielectric environment. Analogous results have been reported for the silica-acetonitrile interface.[8]

Water's extended long range ordering at surfaces and strong, directional hydrogen bonding raise similar questions about how anisotropic water structure impacts water's ability to solvate solutes at interfaces. Studies of structure and dynamics at water-air and water-quartz interfaces have sparked considerable debate as to the dielectric environment, pH, and structural ordering of interfacial water.[9–13] Despite considerable interest in the interfacial water's layering structure, surprisingly little work has considered the effect of water's unique structure at silica interfaces on the solvent's ability to solvate adsorbed solutes.[14–16] In this context, the term solvation

refers explicitly to noncovalent interactions between an adsorbed solute and its surrounding solvent. These interactions can be either nonspecific such as those described by polarizable continuum models or specific such as the localized, directional interactions including hydrogen bonding and other dipole-dipole attractions.[17–20]

A recent report examining the time resolved emission of Coumarin 152 (C152), a solvatochromic fluorescent dye, adsorbed at the silica-aqueous (pH 5.9) interface suggested that adsorbed solutes sampled a distinctly nonpolar solvation environment.[21] Specifically, fluorescence lifetimes measured from the silica-aqueous interface in a total internal reflection (TIR) geometry showed that C152 had a long-lived contribution more typical of C152 solvated in nonpolar solvents such as alkanes or carbon tetrachloride. Coumarin 152 (Fig. 1) derives its solvatochromic behavior from the +4 D change in dipole[22,23] and the proposed formation of a twisted intermolecular charge transfer (TICT) state upon photoexcitation.[24,25] Stabilization of the TICT state by polar, protic solvents is believed to lead to a much shorter fluorescence lifetime and a red shift in the fluorescence spectrum relative to C152's longer (~4 ns) lifetime and shorter wavelength emission in nonpolar media (Fig. 2).[22]

While several density functional theory (DFT) studies[26,27] have questioned whether or not 7-aminocoumarin solutes are likely to form charge transfer states, these calculations did not consider explicitly the role(s) played by individual solvent molecules in stabilizing C152 excited state conformers. Subsequent reports, both experimental[22] and computational,[28] have identified the importance of polar solvents in stabilizing excited TICT state conformations. The excited state photophysical behavior of C152 (and other 7-aminocoumarin solutes) with push/pull functional groups[29,30] in condensed phases is admittedly complicated, and more targeted studies may clarify the excited state structure and dynamics in specific environments. Nevertheless, for the findings reported below, we interpret the time dependent emission behavior of C152 adsorbed to a strongly associating silica-aqueous interface to reflect a restricted solvation environment similar to what C152 experiences in ice.[21]

Given that water and silica are both polar materials, the existence of a "nonpolar" fluorescence lifetime at the silica-aqueous interface is surprising. Two possible explanations for this behavior have been proposed: (1) the effective static dielectric constant at the aqueous-silica interface was reduced from its value in bulk water of 80.4, consistent with reports from studies of water in confined spaces[10] or (2) strong hydrogen bonding between water and the silica substrate restricted interfacial water's mobility so that solvent molecules at the surface could not reorganize around photoexcited

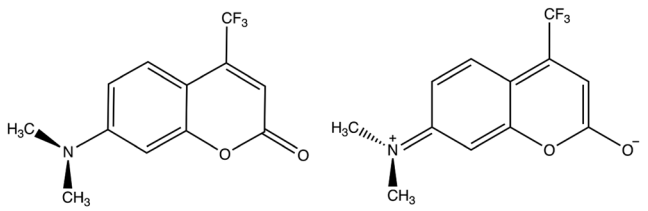

FIG. 1. Structures of Coumarin 152 in its ground state (left) and the excited TICT state (right).

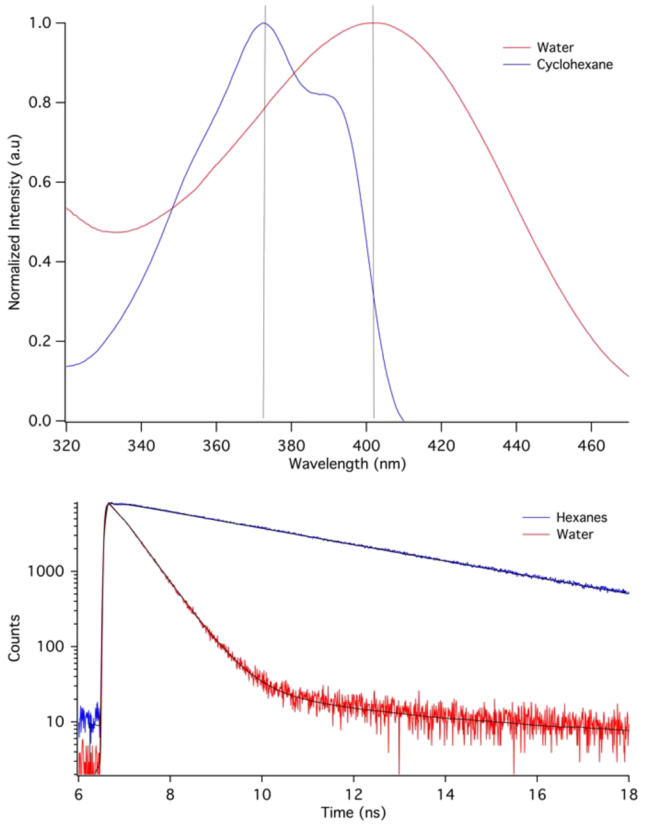

FIG. 2. Top: UV-vis absorbance spectra of C152 in cyclohexane (blue) and water (red). Bottom: TCSPC decay curves for C152 in water (red) and in hexanes (blue). Included in the time resolved emission are fits to exponential decays. Results from these fits are reported in Table I.

C152 to stabilize the TICT state, leading to a longer fluorescence lifetime.[31,32]

Additional studies in the same report measured the fluorescence behavior of C152 frozen in an ice matrix and reported lifetimes consistent with the interfacial TIR measurements. These data implied that restricted solvation dynamics prevented C152 from isomerizing into a nonradiative TICT state upon photoexcitation and bolstered an explanation that solvation at silica-aqueous interfaces was controlled largely by immobilized solvent.

Interpretation of TIR time-resolved fluorescence measurements is hampered by ambiguity about the solutes being excited. Given that fluorescence is not intrinsically surface specific and that the evanescent field of incident light propagates ~150 nm into the adjacent aqueous phase in the TIR geometry used in previous studies, one cannot unambiguously correlate observed solute responses directly to those solutes adsorbed to the solid-liquid interface. In order to resolve whether or not the silica-aqueous interface is truly nonpolar (with a low effective static dielectric constant) *or* if interfacial solvation is due to restricted solvent motion, experiments must be able to discriminate responses from solutes in the interfacial region from those originating in the adjacent, isotropic bulk. With this consideration in mind, resonance enhanced second harmonic

generation (SHG) is a valuable and complementary tool for testing predictions that emerged from the TIR time-resolved emission studies. SHG is intrinsically sensitive only to molecules subject to the anisotropy induced by an interface within the electric dipole limit.[33–35] Furthermore, SHG's sensitivity to electronic resonances makes it ideally well suited for probing the local equilibrium solvation environment sampled by C152 adsorbed to the silica-water interface.

Data presented below report resonance enhanced SHG spectra from C152 molecules adsorbed to the silica-water interface. Results show that C152's effective excitation wavelength at the silica-aqueous interface is slightly longer than that in bulk aqueous solution, supporting the idea that solvation at the silica-aqueous interface is characterized by a high permittivity. This result, together with C152's time resolved emission, shows that solvation at the strongly associating silica-water interface is characterized by high local polarity and restricted solvent mobility. Disrupting substrate-solvent association changes the local solvation environment dramatically. SHG and time resolved fluorescence data acquired from C152 molecules adsorbed to a *hydrophobic* silica-water interface show a local dielectric environment similar to what one would expect if interfacial solvation were described by averaged contributions from the adjacent phases. Complementary SHG and time resolved emission data illustrate that strong solvent-substrate association can conspire to create conflicting pictures of equilibrium and dynamic solvation.

II. EXPERIMENTAL

Laser grade Coumarin 152 was purchased and used as received from exciton. Water used in the experiments was nanopure, from a Millipore filtration system, a resistivity of 18.2 MΩ and a surface tension of 72.3 mN/m at 22 °C. Silica slides and experimental assemblies were rinsed with methanol and de-ionized (DI) water then soaked in a bath of 50/50 sulfuric/nitric acid for no less than 1 hr and rinsed with DI water and dried under nitrogen before use. Experiments described in this work used saturated solutions of Coumarin 152 in water that were made by combining excess C152 and water and allowing the solution to equilibrate with stirring overnight at 50 °C. The solutions were filtered to remove excess dye before use. At room temperature, the concentration of C152 in a saturated aqueous solution is approximately 6 μM. SHG spectra were collected from Kel-F sample chambers containing saturated C152 solution in contact with fused silica slides (Structure Probe, Inc.). For total internal reflection-time-correlated single-photon counting (TIR-TCSPC) measurements, a custom-built assembly was made from Kel-F sample chambers containing saturated aqueous C152 solution in contact with fused silica prisms (ISP Optics, Inc.) that allowed the excitation pulse to irradiate the interface formed between a hemispherical prism and an aqueous solution at angles greater than the critical angle (61° at 400 nm). Sample chambers, coumarin solutions, silica slides, and prisms were allowed to equilibrate for at least an hour before being used in experiments.

Silica slides (Structure Probe, Inc.) and prisms (ISP Optics, Inc.) were functionalized according to previously published methods[36,37] with a solution of dimethyldichlorosilane in toluene to create hydrophobic surfaces. These methods have been shown to reproduce consistent hydrophobic monolayers on a silica substrate. Silica substrates were cleaned as described above and allowed to sit in a 3% silane solution at 130 °C for 36 h. This procedure reliably leads to water contact angles of 100°. Once removed from the silane solution, silica slides and prisms were first washed with toluene, then methanol, and finally tested with water to verify that the surface was hydrophobic. Slides were used within 24 h of silanization to ensure consistency of the monolayer.

To collect TIR-TCSPC spectra, the output of a Ti:Sapphire oscillator (Chameleon, Coherent) was frequency doubled (APE Autotracker) and the 80 MHz repetition rate was attenuated to 4 MHz using an electro-optic modulator (Conoptics Model 350-105). Fluorescence emission was collected using a Picoquant 200 time-to-amplitude converter, and the instrument response function (IRF) was measured using a nonemissive Ludox scattering solution. Emission was detected at 90° relative to the silica-aqueous interface. The TIR assembly's IRF was ~200 ps. For every experiment, the IRF was deconvoluted from the time-resolved emission histogram and the resulting trace was then fit to one or more single exponential decays. The minimum number of lifetimes required to accurately fit the data was determined using the Akaike information criterion.[38]

In order to collect the SHG signal from surface molecules, the coherent output from a tunable, amplified Ti:sapphire pumped optical parametric amplifier (OPA) at frequency ω is focused on the surface and creates a polarization of the surface molecules at 2ω. The intensity of the collected second harmonic signal is proportional to the square of the second order polarizability, denoted as $P^{(2)}$

$$I(2\omega) \propto \left|P^{(2)}(2\omega)\right|^2, \tag{1}$$

where $P^{(2)} = \left|\chi^{(2)}E(\omega_1)E(\omega_2)\right|$. In the case of second harmonic generation, the incident beam is of a single frequency and $\omega_1 = \omega_2$. The surface specificity of SHG, along with all second order nonlinear optical techniques, derives from $\chi^{(2)}$, the second order nonlinear susceptibility. $\chi^{(2)}$ is a rank 3 tensor consisting of 27 matrix elements; in centrosymmetric systems, the requirement that $\chi^{(2)}_{i,j,k} = \chi^{(2)}_{-i,-j,-k}$ means that no second harmonic response will originate from an isotropic solution within the electric dipole approximation. At an interface where symmetry is broken, elements of the $\chi^{(2)}$ tensor can take on nonzero values, dependent on the identity of the molecules at the interface. $\chi^{(2)}$ is composed of a nonresonant (NR) piece and a resonant (R) piece

$$\chi^{(2)} = \chi^{(2)}_{NR} + \chi^{(2)}_{R}. \tag{2}$$

The nonresonant portion of the $\chi^{(2)}$ tensor is usually simple and can be fit to a single value, whereas the resonant contribution is more complicated. The resonant portion of $\chi^{(2)}$ is equal to the number of molecules on the surface multiplied by the orientational average over the molecular hyperpolarizability (β) of the adsorbed molecules

$$\chi^{(2)}_R = N\langle\beta_{i,j,k}\rangle, \quad \text{where } \beta \text{ is given by } \beta = \frac{A}{\omega_0 - \omega - i\Gamma}. \tag{3}$$

In this expression for β, A is a constant related to the transition dipole moment of the electronic resonance being examined, ω_0 is

the resonant frequency of the transition, ω is the frequency of the incident light, and Γ is the linewidth associated with the transition.

In cases where the interface under investigation carries a surface charge, the second harmonic spectral lineshape can be influenced by some nonresonant elements of the $\chi^{(3)}$ tensor, which makes Eq. (2) take the form

$$\chi^{(2)}_{total} \propto \chi^{(2)} + (\chi^{(3)}_1 + i\chi^{(3)}_2)\Phi(0), \quad (4)$$

where Φ(0) is the interfacial potential and both elements of the $\chi^{(3)}$ tensor are purely real.[39,40] Collected second harmonic spectra are fit with Eqs. (2)–(4) to determine the linewidth and the center of the resonant peak.

Resonance-enhanced SHG spectra were acquired from an experimental assembly that has been described previously.[41,42] Briefly, ~3.3 W from a Ti:Sapphire regenerative amplifier (Libra-HE, Coherent, 85 fs pulses, 1 kHz repetition rate, 801 nm) was coupled to a visible optical parametric amplifier (Coherent OPerA Solo, FWHM 10 nm) and focused on the sample. If necessary, incident visible light was attenuated to below 4 mW with neutral density filters before it reached the sample. The second harmonic signal was collected using a photomultiplier tube and photon counting electronics. Data from each individual wavelength were collected over 3–5 separate 10 s intervals, background corrected, and then averaged. Typically, up to 300 counts were measured on resonance during a 10 s acquisition.

III. RESULTS AND DISCUSSION

Figure 3 shows the second harmonic spectrum of C152 at the silica/aqueous interface. Also included on the opposite ordinate is C152's absorbance spectrum in bulk water. The SHG data show that the surface spectrum experiences a modest bathochromic shift relative to the spectrum in bulk water, with the resonance center at the surface measuring 405 nm, 7 nm higher than the absorbance peak at

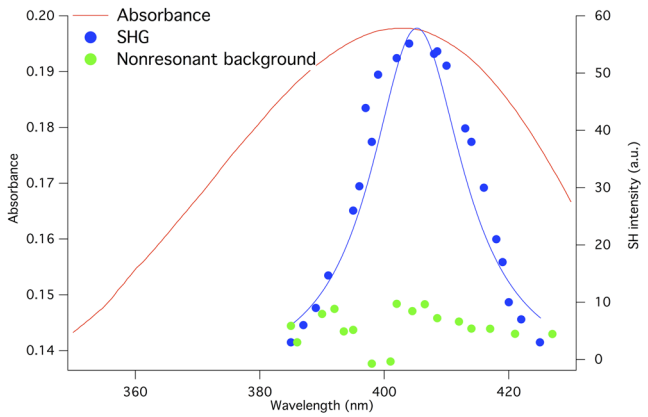

FIG. 3. UV-vis absorbance of C152 in water (red) and the surface second harmonic spectrum of C152 at the water-silica interface (blue). Also included are SHG data from the water-silica interface in the absence of any adsorbed C152 (green) emphasizing C152's strong resonant enhancement of the SHG response. SHG data are fit to Eqs. (1)–(4), and the results of this fitting procedure are included as the blue, solid line.

398 nm in bulk aqueous solution. This result includes the $\chi^{(3)}$ term in Eq. (4) above with an assumed surface potential of 70–80 mV given an unbuffered, pH = 6 aqueous solution.[39,40,43] [Omitting the $\chi^{(3)}$ contribution changes the calculated excitation wavelength maximum by less than 1.5 nm.] According to C152's well-characterized solvatochromic behavior, a red-shifted spectrum implies solvation in a more polar dielectric environment.[22] This result at the water-silica interface is consistent with experiments and calculations predicting that water molecules immobilized in a solid ice matrix can also create a more polar dielectric environment than that found in liquid water. Under the influence of dipole ordering introduced by the solid structure, ice's dielectric constant is reported to be between 78.2 and 107, depending on the ice structure and temperature.[44–46] (Pure water at room temperature has a dielectric constant of 80.4.)

Both experimental and computational results have shown that water molecules within 10 Å of a silica surface experience a hexagonal ordering analogous to water molecules frozen in a solid state.[47–49] The alignment of dipoles at the surface induces the coumarin to display spectroscopic evidence of a more polar *static*, dielectric environment at the surface than in bulk. At the silica-aqueous interface, all of the water dipoles are expected to be aligned in the same direction for the first 2–3 solvent layers.[47,50] We propose that this anisotropic solvent dipole ordering leads to a local permittivity greater than that of an isotropic arrangement of the same solvent in bulk solution. Given these considerations, the fluorescence signatures reported in Ref. 21 are unlikely to originate from any sort of nonpolar environment (with an effective alkane-like static dielectric constant). Instead, since the SHG spectrum of the silica-aqueous interface implies that water's molecular dipoles are highly structured due to strong association with the silica substrate creating a large effective dielectric constant, a more likely explanation for the long lifetime in C152 fluorescence is that restricted solvent reorientation dynamics are too slow to enable formation of the C152's nonradiative TICT state. Taken together, the SHG data imply a very polar static environment but the TIR (and bulk ice) fluorescence measurements suggest slower dynamic solvation than found in bulk solution. These results should not be surprising given interfacial water rotational correlation times reported to be as much as 40 times slower at the surface than in bulk solution.[31,32]

At the silica-aqueous interface, time-resolved fluorescence spectra of C152 show a very long fluorescence lifetime, generally resulting from C152 solvated in nonpolar solvents such as alkanes. Since the SHG results presented here confirm that the silica-aqueous interface is indeed polar, we conclude that the fluorescence results derive from restricted solvation at the interface and not from any reduction in the interfacial static polarity. Furthermore, if this description is accurate, we expect that disrupting the ability of water to hydrogen bond to the silica surface will cause the static solvation environment sampled in SHG experiments and the time-dependent solvation interactions probed by TIR-time resolved fluorescence to be more consistent with each other.

In order to disrupt the strong ordering effects of the silica surface on the adjacent water structure and dynamics, we functionalized silica slides with a dichlorodimethylsilane to create nonpolar, methyl terminated silica surfaces[36,37] and performed SHG and TIR-TCSPC measurements of C152 adsorbed to this hydrophobic silica-water boundary. Figure 4 shows the SHG spectrum of

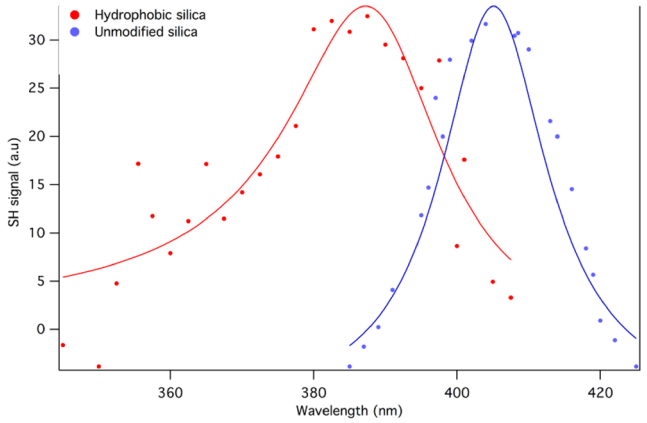

FIG. 4. SHG spectra of C152 at the hydrophilic (blue) and hydrophobic (red) silica interface. SHG data are fit to Eqs. (1)–(4), and the results of this fitting procedure are included as the red and blue solid lines.

C152 adsorbed to the hydrophobic silica-aqueous interface. The same SHG spectrum of C152 adsorbed to the *hydrophilic* silica-aqueous interface first shown in Fig. 2 is reproduced for comparison. At the hydrophobic-aqueous interface, C152's SHG spectrum shows strong resonance enhancement with an excitation wavelength maximum of 389 nm, considerably blue-shifted from the 405 nm measured at the unmodified hydrophilic silica-aqueous surface and from the 398 nm measured in bulk aqueous solution. This hydrophobic silica-aqueous excitation wavelength is consistent with a local solvation environment similar to that found in bulk polar organic solvents such as ethyl acetate and acetone.[22] Furthermore, this result is also consistent with expectations that a hydrophobic surface and a polar solvent would create an interfacial solvation environment that reflected averaged contributions from the two phases.[2,51]

The SHG spectrum acquired from this hydrophobic-aqueous interface is broader than that measured at the unmodified silica-aqueous interface, with a linewidth of 26 nm compared to 19 nm at the hydrophilic interface. This spectral broadening often indicates a heterogeneous solvation environment.[52] The fact that the linewidth for C152 at the unmodified silica interface is narrower than that at the hydrophobic interface implies that the unmodified silica-water interface exhibits some degree of order that prevents further inhomogeneous broadening relative to what is observed at the hydrophobic interface. While film defects or unmodified patches of the silica slide would also result in a more heterogeneous solvation environment, we would expect these effects to manifest themselves as C152 solvation at a polar, strongly associating silica-aqueous interface similar to the data shown in Fig. 3 (and reproduced in Fig. 4). SHG data from the hydrophobic silica-aqueous interface do not support an interpretation based on an inhomogeneous hydrophobic film.

The SHG data show clearly that C152 adsorbed to the hydrophobic silica-aqueous interface samples a less polar environment, indicating that disrupting the strong substrate-solvent interactions diminishes the local polarity. The consequences of this disrupted interfacial solvent structure on C152's time dependent emission behavior can also be observed in the TIR-TCSPC measurements shown in Fig. 5. These experiments were performed using hemispherical silica prisms that had been functionalized with dimethylsilane in the same manner as the silica slides used for SHG experiments. Also shown in Fig. 5 for comparison is the time-resolved fluorescence from C152 adsorbed to the hydrophilic silica-aqueous interface.

As previously reported, a saturated solution of C152 in water at the unmodified silica-aqueous interface shows evidence of two fluorescence lifetimes—87% of the decay corresponds to C152 solvents in contact with bulk water with a lifetime of 0.47 ns and 13% from solutes in contact with the silica surface with a lifetime of 3.52 ns.[21] The longer lifetime is similar to C152's single, ~4 ns lifetime in nonpolar media. At the hydrophobic silica-aqueous interface, fluorescence decays cannot be fit with fewer than 3 lifetimes. 72% of the decay still derives from C152 solutes dissolved in bulk water solution, with a lifetime of 0.45 ns. 4% of the decay fits to a longer fluorescence lifetime of 4.25 ns, either from solutes held by hydrogen bonds at defects in the hydrophobic surface layer or from molecules completely excluded from water by the nonpolar molecules on the silica surface. The third lifetime seen at this interface comprises 24% of the total decay and corresponds to a new lifetime of 0.93 ns, typically attributed to C152 in a polar, hydrogen bonding solvent similar to methanol. This additional lifetime is necessary to adequately fit the fluorescence data from the hydrophobic silica-aqueous interface as the χ^2 value for the 2-exponent fit is 2.701, while adding the 3rd exponent improves the χ^2 result to 1.024. These results are summarized in Table I. Considering the structure of the hydrophobic silica-aqueous interface, this additional lifetime is sensible. The

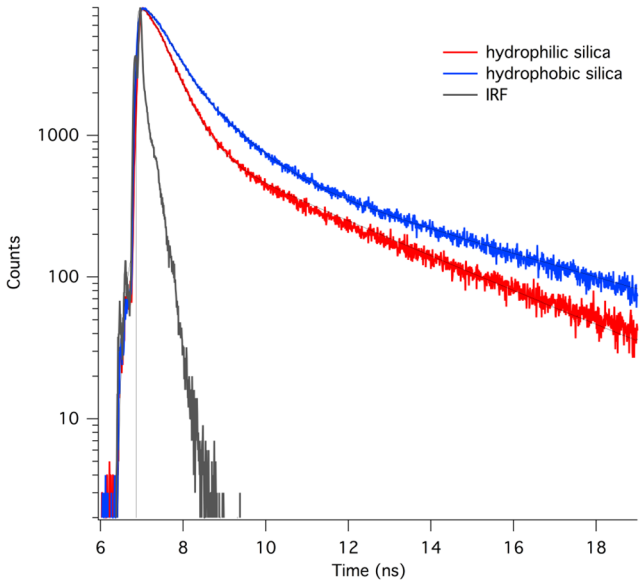

FIG. 5. TIR-TCSPC traces of C152 at the hydrophobic silica-aqueous interface (blue) and hydrophilic silica-aqueous interface (red). Results from fitting these data to independent exponential decays are reported in Table I. The instrument response function (IRF) from a scattering, nonemissive solution of Ludox is included for reference (black trace).

TABLE I. Fluorescence lifetimes and amplitudes of C152 adsorbed to aqueous-hydrophilic and aqueous-hydrophobic interfaces as measured by TIR-TCSPC. Lifetime data assigned to bulk solvated solutes are reported as A_1 and τ_1.

	A_1 (%)	τ_1 (ns) (bulk)	A_2 (%)	τ_2 (ns) (nonpolar)	A_3 (%)	τ_3 (ns) (polar protic)
Hydrophobic silica	72	0.45	4	4.25	24	0.93
Hydrophilic silica	87	0.47	13	3.52	n/a	n/a

silica surface is composed of a layer of terminal methyl groups, and the interfacial water solvent is expected to diminish in density and to be considerably less ordered.[53,54]

The additional lifetime also makes the SHG and TIR-TCSPC results from the hydrophobic interface much more internally consistent relative to the apparently conflicting findings from the hydrophilic interface. The SHG results at the hydrophobic silica interface indicate a dielectric environment similar to that of bulk acetone ($\varepsilon = 20.7$), while the time-resolved fluorescence data indicate a polar, protic solvation environment similar to that of methanol.

IV. CONCLUSIONS

The results presented in this work create a more nuanced picture of water's solvation properties at hydrophilic and hydrophobic silica-aqueous interfaces. Previous results indicated that solute isomerization was impeded at hydrophilic silica-aqueous interfaces and implied that the interface had distinctive nonpolar character. Resonance enhanced SHG spectra of adsorbed C152 show that the hydrophilic silica-aqueous interface is, in fact, characterized by a strong local dielectric constant. The restricted solute isomerization, then, likely reflects slower solvent reorientation dynamics resulting from strong water-silica association. Disrupting these solvent-substrate interactions leads to static and dynamic interfacial solvation properties that more closely mirror each other.

ACKNOWLEDGMENTS

The authors gratefully acknowledge support from the National Science Foundation [Grant Nos. 1710695 (G.E.P.) and 1757351 (R.A.W.)]. The authors thank Dr. Charles Stark and Dr. Christine Gobrogge for assistance with the initial TCSPC measurements. The authors also thank Professor Franz Geiger for helpful discussions and computational assistance to determine the role played by $\chi^{(3)}$ on resonance enhanced SHG spectra.

No competing financial interests have been declared.

REFERENCES

[1] Q. Du, R. Superfine, E. Freysz, and Y. R. Shen, "Vibrational spectroscopy of water at the vapor water interface," Phys. Rev. Lett. **70**(15), 2313–2316 (1993).
[2] H. F. Wang, E. Borguet, and K. B. Eisenthal, "Polarity of liquid interfaces by second harmonic generation spectroscopy," J. Phys. Chem. A **101**(4), 713–718 (1997).
[3] W. H. Steel, C. L. Beildeck, and R. A. Walker, "Solvent polarity across strongly associating interfaces," J. Phys. Chem. B **108**(41), 16107–16116 (2004).
[4] F. Reymond, D. Fermin, H. J. Lee, and H. H. Girault, "Electrochemistry at liquid/liquid interfaces: Methodology and potential applications," Electrochim. Acta **45**(15-16), 2647–2662 (2000).
[5] X. Y. Zhang and R. A. Walker, "Discrete partitioning of solvent permittivity at liquid-solid interfaces," Langmuir **17**(15), 4486–4489 (2001).
[6] W. H. Steel and R. A. Walker, "Measuring dipolar width across liquid-liquid interfaces with 'molecular rulers,'" Nature **424**(6946), 296–299 (2003).
[7] D. Roy, S. L. Liu, B. L. Woods, A. R. Siler, J. T. Fourkas, J. D. Weeks, and R. A. Walker, "Nonpolar adsorption at the silica/methanol interface: Surface mediated polarity and solvent density across a strongly associating solid/liquid boundary," J. Phys. Chem. C **117**(51), 27052–27061 (2013).
[8] B. J. Berne, J. T. Fourkas, R. A. Walker, and J. D. Weeks, "Nitriles at silica interfaces resemble supported lipid bilayers," Acc. Chem. Res. **49**(9), 1605–1613 (2016).
[9] K. Leung, I. M. B. Nielsen, and L. J. Criscenti, "Elucidating the bimodal acid-base behavior of the water-silica interface from first principles," J. Am. Chem. Soc. **131**(51), 18358–18365 (2009).
[10] L. Fumagalli, A. Esfandiar, R. Fabregas, S. Hu, P. Ares, A. Janardanan, Q. Yang, B. Radha, T. Taniguchi, K. Watanabe, G. Gomila, K. S. Novoselov, and A. K. Geim, "Anomalously low dielectric constant of confined water," Science **360**(6395), 1339–1342 (2018).
[11] S. Nihonyanagi, S. Yamaguchi, and T. Tahara, "Water hydrogen bond structure near highly charged interfaces is not like ice," J. Am. Chem. Soc. **132**(20), 6867–6869 (2010).
[12] M. D. Boamah, P. E. Ohno, F. M. Geiger, and K. B. Eisenthal, "Relative permittivity in the electrical double layer from nonlinear optics," J. Chem. Phys. **148**(22), 222808 (2018).
[13] L. Dalstein, E. Potapova, and E. Tyrode, "The elusive silica/water interface: Isolated silanols under water as revealed by vibrational sum frequency spectroscopy," Phys. Chem. Chem. Phys. **19**(16), 10343–10349 (2017).
[14] G. L. Richmond, "Molecular bonding and interactions at aqueous surfaces as probed by vibrational sum frequency spectroscopy," Chem. Rev. **102**(8), 2693–2724 (2002).
[15] J. A. Mondal, S. Nihonyanagi, S. Yamaguchi, and T. Tahara, "Structure and orientation of water at charged lipid monolayer/water interfaces probed by heterodyne-detected vibrational sum frequency generation spectroscopy," J. Am. Chem. Soc. **132**(31), 10656–10657 (2010).
[16] O. Isaienko and E. Borguet, "Hydrophobicity of hydroxylated amorphous fused silica surfaces," Langmuir **29**(25), 7885–7895 (2013).
[17] M. R. Brindza and R. A. Walker, "Differentiating solvation mechanisms at polar solid/liquid interfaces," J. Am. Chem. Soc. **131**(17), 6207–6214 (2009).
[18] S. Shin and A. P. Willard, "Water's interfacial hydrogen bonding structure reveals the effective strength of surface-water interactions," J. Phys. Chem. B **122**(26), 6781–6789 (2018).
[19] F. Zaera, "Probing liquid/solid interfaces at the molecular level," Chem. Rev. **112**(5), 2920–2986 (2012).
[20] Z. Sohrabpour, P. M. Kearns, and A. M. Massari, "Vibrational sum frequency generation spectroscopy of fullerene at dielectric interfaces," J. Phys. Chem. C **120**(3), 1666–1672 (2016).
[21] G. E. Purnell and R. A. Walker, "Hindered isomerization at the silica/aqueous interface: Surface polarity or restricted solvation?," Langmuir **34**(34), 9946–9949 (2018).

[22]S. Nad, M. Kumbhakar, and H. Pal, "Photophysical properties of coumarin-152 and coumarin-481 dyes: Unusual behavior in nonpolar and in higher polarity solvents," J. Phys. Chem. A **107**(24), 4808–4816 (2003).
[23]P. Dahiya, M. Kumbhakar, T. Mukherjee, and H. Pal, "Effect of protic solvents on twisted intramolecular charge transfer state formation in coumarin-152 and coumarin-481 dyes," Chem. Phys. Lett. **414**(1-3), 148–154 (2005).
[24]J. E. T. Corrie, V. R. N. Munasinghe, and W. Rettig, "Synthesis and fluorescence properties of substituted 7-aminocoumarin-3-carboxylate derivatives," J. Heterocycl. Chem. **37**(6), 1447–1455 (2000).
[25]T. L. Arbeloa, F. L. Arbeloa, M. J. T. Estevez, and I. L. Arbeloa, "Binary solvent effects on the absorption and emission of 7-aminocoumarins," J. Lumin. **59**(6), 369–375 (1994).
[26]R. J. Cave and E. W. Castner, "Time-dependent density functional theory investigation of the ground and excited states of coumarins 102, 152, 153, and 343," J. Phys. Chem. A **106**(50), 12117–12123 (2002).
[27]R. J. Cave, K. Burke, and E. W. Castner, "Theoretical investigation of the ground and excited states of Coumarin 151 and Coumarin 120," J. Phys. Chem. A **106**(40), 9294–9305 (2002).
[28]A. Pedone, "Role of solvent on charge transfer in 7-aminocoumarin dyes: New hints from TD-CAM-B3LYP and state specific PCM calculations," J. Chem. Theory Comput. **9**(9), 4087–4096 (2013).
[29]Z. R. Grabowski, K. Rotkiewicz, and W. Rettig, "Structural changes accompanying intramolecular electron transfer: Focus on twisted intramolecular charge-transfer states and structures," Chem. Rev. **103**(10), 3899–4031 (2003).
[30]K. Rechthaler and G. Kohler, "Excited-state properties and deactivation pathways of 7-aminocoumarins," Chem. Phys. **189**(1), 99–116 (1994).
[31]A. A. Milischuk and B. M. Ladanyi, "Structure and dynamics of water confined in silica nanopores," J. Chem. Phys. **135**(17), 174709 (2011).
[32]M. R. Warne, N. L. Allan, and T. Cosgrove, "Computer simulation of water molecules at kaolinite and silica surfaces," Phys. Chem. Chem. Phys. **2**(16), 3663–3668 (2000).
[33]N. Bloembergen, "2nd harmonic reflected light," Opt. Acta **13**(4), 311–322 (1966).
[34]K. B. Eisenthal, "Second harmonic spectroscopy of aqueous nano- and microparticle interfaces," Chem. Rev. **106**(4), 1462–1477 (2006).
[35]T. F. Heinz, C. K. Chen, D. Ricard, and Y. R. Shen, "Spectroscopy of molecular monolayers by resonant 2nd-harmonic generation," Phys. Rev. Lett. **48**(7), 478–481 (1982).
[36]X. Y. Zhang, O. Esenturk, and R. A. Walker, "Reduced polarity in protic solvents near hydrophobic solid surfaces," J. Am. Chem. Soc. **123**(43), 10768–10769 (2001).
[37]P. Horng, M. R. Brindza, R. A. Walker, and J. T. Fourkas, "Behavior of organic liquids at bare and modified silica interfaces," J. Phys. Chem. C **114**(1), 394–402 (2010).
[38]E. Bajzer, M. C. Moncrieffe, I. Penzar, and F. G. Prendergast, "Complex homogeneous and heterogeneous fluorescence anisotropy decays: Enhancing analysis accuracy," Biophys. J. **81**(3), 1765–1775 (2001).
[39]P. E. Ohno, H. F. Wang, and F. M. Geiger, "Second-order spectral lineshapes from charged interfaces," Nat. Commun. **8**, 1032 (2017).
[40]P. E. Ohno, S. A. Saslow, H. F. Wang, F. M. Geiger, and K. B. Eisenthal, "Phase-referenced nonlinear spectroscopy of the alpha-quartz/water interface," Nat. Commun. **7**, 13587 (2016).
[41]B. L. Woods and R. A. Walker, "pH effects on molecular adsorption and solvation of *p*-nitrophenol at silica/aqueous interfaces," J. Phys. Chem. A **117**(29), 6224–6233 (2013).
[42]B. L. Woods, J. K. George, A. M. Sherman, P. R. Callis, and R. A. Walker, "Adsorption and aggregation at silica/methanol interfaces: The role of solute structure," J. Phys. Chem. C **119**(25), 14230–14238 (2015).
[43]B. M. Lowe, C. K. Skylaris, N. G. Green, Y. Shibuta, and T. Sakata, "Calculation of surface potentials at the silica-water interface using molecular dynamics: Challenges and opportunities," Jpn. J. Appl. Phys. **57**(4S), 04FM02 (2018).
[44]J. L. Aragones, L. G. MacDowell, and C. Vega, "Dielectric constant of ices and water: A lesson about water interactions," J. Phys. Chem. A **115**(23), 5745–5758 (2011).
[45]G. P. Johari and E. Whalley, "The dielectric-properties of ice Ih in the range 272–133 K," J. Chem. Phys. **75**(3), 1333–1340 (1981).
[46]S. W. Rick and A. D. J. Haymet, "Dielectric constant and proton order and disorder in ice Ih: Monte Carlo computer simulations," J. Chem. Phys. **118**(20), 9291–9296 (2003).
[47]Y. R. Shen and V. Ostroverkhov, "Sum-frequency vibrational spectroscopy on water interfaces: Polar orientation of water molecules at interfaces," Chem. Rev. **106**(4), 1140–1154 (2006).
[48]Q. Du, E. Freysz, and Y. R. Shen, "Vibrational-spectra of water-molecules at quartz water interfaces," Phys. Rev. Lett. **72**(2), 238–241 (1994).
[49]M. Bouhadja and A. A. Skelton, "Dynamical properties of water and ions at the quartz (101)-water interface at a range of solution conditions: A classical molecular dynamics study," J. Phys. Chem. C **122**(3), 1535–1546 (2018).
[50]P. K. Gupta and M. Meuwly, "Dynamics and vibrational spectroscopy of water at hydroxylated silica surfaces," Faraday Discuss. **167**, 329–346 (2013).
[51]H. F. Wang, E. Borguet, and K. B. Eisenthal, "Generalized interface polarity scale based on second harmonic spectroscopy," J. Phys. Chem. B **102**(25), 4927–4932 (1998).
[52]I. Benjamin, "Inhomogeneous broadening of electronic spectra at liquid interfaces," Chem. Phys. Lett. **515**(1-3), 56–61 (2011).
[53]E. Tyrode and J. F. D. Liljeblad, "Water structure next to ordered and disordered hydrophobic silane monolayers: A vibrational sum frequency spectroscopy study," J. Phys. Chem. C **117**(4), 1780–1790 (2013).
[54]S. H. Lee and P. J. Rossky, "A comparison of the structure and dynamics of liquid water at hydrophobic and hydrophilic surfaces—A molecular-dynamics simulation study," J. Chem. Phys. **100**(4), 3334–3345 (1994).